BMC Oral Health

RESEARCH

Open Access

Benzo[a]pyrene exposure affect the formation of dental hard tissue via the regulation of glycerophospholipid metabolism

Yue Pan[1], Sihan Yu[2], Xinyuan Feng[1], Yiran Zhao[1], Dixin Cui[3] and Xiaoyan Wang[1*]

Abstract

Background The formation of enamel occurs across multiple developmental stages and is highly sensitive to disruptions in cellular signaling. Perinatal complications, preterm birth, and exposure to environmental chemicals are systemic factors known to contribute to developmental defects of enamel (DDE). These defects adversely affect normal oral physiological function and impact patients' daily lives. The precise pathophysiology of DDE, however, remains unclear, complicating efforts at prevention. Consequently, elucidating the mechanisms through which environmental exposures lead to DDE is essential for developing preventive and early intervention strategies to support lifelong oral health.

Methods Sprague Dawley (SD) rats received daily intraperitoneal injections of 5 μg/kg benzo[a]pyrene (B[a]P) from postnatal day 1 to day 42 to establish the DDE model. At postnatal week 6, we performed phenotypic analysis using dual-platform untargeted metabolomics, transcriptomics sequencing, hematological examination, and micro-CT. Statistical evaluation of all data employed Student's t-tests or one-way ANOVA with Tukey's post hoc test ($P < 0.05$).

Results B[a]P exposure shortened molar crowns and induced abnormal pits on the lingual side of incisors, indicating disrupted tooth development through micro-CT analysis. It also reduced incisor enamel volume and density, leading to a DDE phenotype. This enamel defect coincided with hepatic metabolic disorders and an upregulation of phospholipid metabolism. Throughout DDE progression, differentially enriched metabolites within phospholipid pathways were observed in dental epithelial cells concurrently with reduced transcriptional levels of enamel formation genes.

Conclusions This study established a rat model of DDE and demonstrated the multifaceted impacts of B[a]P exposure on both tooth development and systemic metabolism, revealing a correlation between altered phospholipid metabolism and transcriptional changes in enamel formation-related genes. These findings provide the first evidence linking glycerophospholipid metabolism to exposure-induced DDE and suggest its potential relevance for DDE prevention. This work provides further theoretical support for promoting oral health management in early childhood.

Keywords Developmental defects of enamel, Environmental endocrine disruptors, Lipid metabolism disorders

*Correspondence:
Xiaoyan Wang
wangxiaoyanpx@163.com

Full list of author information is available at the end of the article

Graphical Abstract

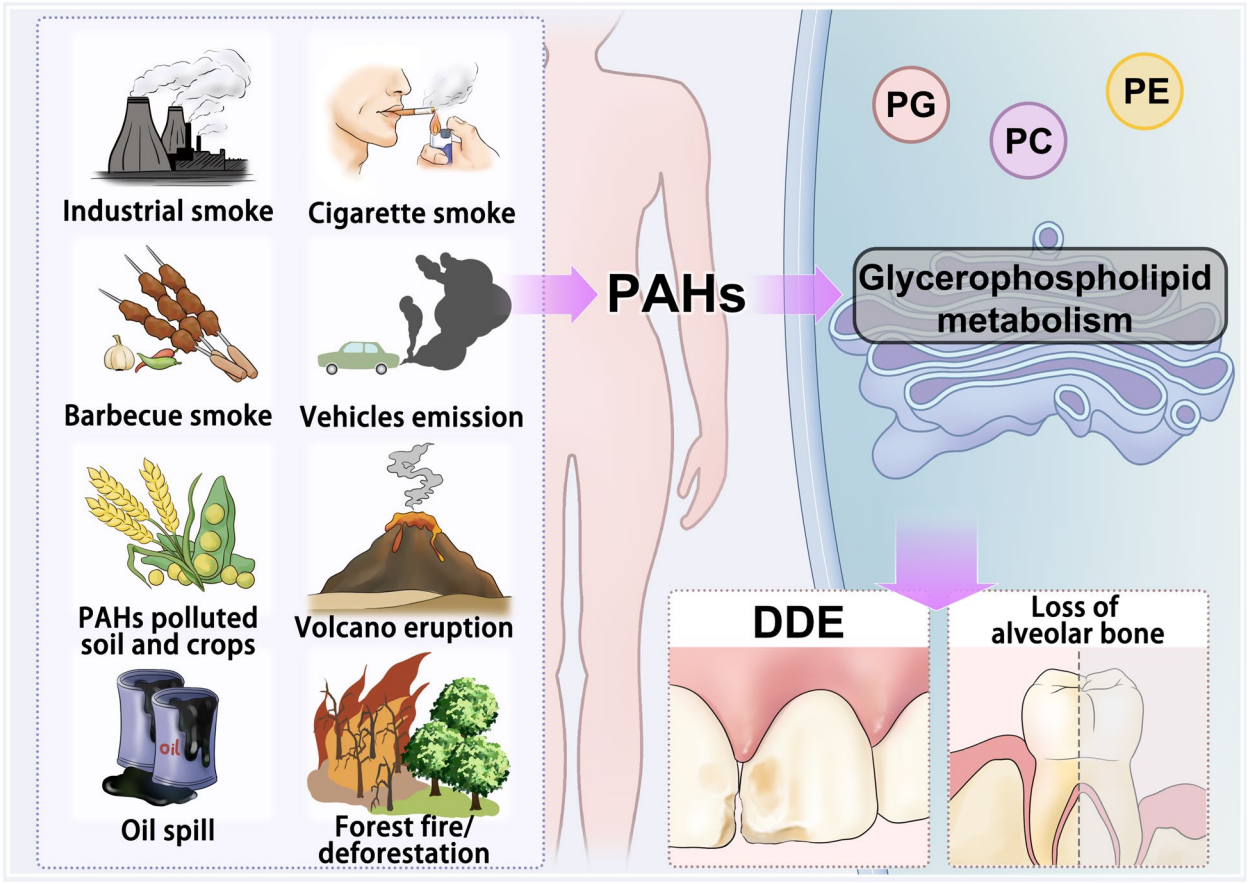

Background

Enamel protects dental hard tissues, facilitates mastication, and contributes to facial aesthetics. Its formation is a prolonged, multi-stage developmental process that is highly vulnerable to signaling disruptions, which can cause developmental defects of enamel (DDE) and impair normal oral function [1]. With a rising trend observed in recent years, the occurrence rate of DDE ranges from 9% to 96% [2, 3], which may be attributed to differences in country, ethnicity, economic development level, and examination methods employed in the respective research. Precise prevention remains difficult, however, due to numerous risk factors and an incompletely understood pathogenesis. Moreover, treatments for affected teeth are frequently complicated by dentin hypersensitivity and suboptimal restoration outcomes. Children with undiagnosed or untreated DDE are at greater risk for oral health complications. A deeper understanding of the etiology and mechanisms underlying DDE is therefore crucial for developing effective prevention and early intervention strategies.

In recent years, the correlation between alterations in individual epigenetic modifications induced by chemical, physical, and biological factors in the environment and the onset of diseases has garnered widespread attention [4, 5]. Previous research demonstrated that exposure to the environmental stimulant bisphenol A leads to developmental defects in the enamel of mouse incisors, resulting in impaired enamel formation and a phenotype resembling human molar-incisor hypomineralisation (MIH) [6]. The enamel formation disorder in mice was accompanied by an enhanced H3K27me3 modification state in dental epithelial stem cells, which impaired stemness maintenance and led to abnormal cell proliferation. Another study, utilizing a mouse model of nicotine exposure during pregnancy, revealed that early-life nicotine exposure can interfere with enamel formation in mice, causing whitish opaque alterations and microstructural disorganization indicative of hypomineralization [7]. These findings suggest that early-life exposure to environmental endocrine disruptors (EEDs) is closely associated with enamel development and the pathogenesis of conditions such as DDE.

Polycyclic aromatic hydrocarbons (PAHs) represent a class of typical persistent organic environmental pollutants and endocrine disruptors. They are widely and persistently present in the human environment, leading to frequent and unavoidable exposure [8]. China is one of the countries with high PAHs emissions globally [9]. Natural sources of PAHs primarily include smoke from forest fires and volcanic eruptions, while anthropogenic sources mainly involve incomplete combustion of organic materials, such as industrial and vehicular emissions, industrial by-products, food processing, and tobacco smoke [10–12]. PAHs constitute the largest group of known carcinogenic compounds, ranking high on the pollutant lists of the European Union and the U.S. Environmental Protection Agency, and are recognized as the ninth most hazardous compounds to human health [13]. The International Agency for Research on Cancer (IARC) classifies PAHs into different categories based on their carcinogenicity. Among them, benzo[a]pyrene (B[a]P) is categorized separately as a Group 1 carcinogen due to its well-established carcinogenic potential and is often used as a reference for evaluating the carcinogenicity of other PAHs [14]. Studies have confirmed that maternal exposure to PAHs can result in the transfer of approximately 25% of the body burden to offspring via breastfeeding [15]. Additionally, accidental high-level exposure to PAHs in children has been associated with developmental enamel defects and permanent tooth loss [16]. High-dose PAHs exposure has been demonstrated to suppress early molar development in rats, reduce molar size, impair mineralization of enamel and dentin, and inhibit root formation [17]. However, the mechanisms by which B[a]P affects dental development and induces enamel abnormalities remain unclear.

Previous studies indicate that the toxicity and carcinogenicity of PAHs may arise from oxidative damage and metabolic dysregulation [18, 19]. In the lungs, PAHs bind to the aryl hydrocarbon receptor, activating Phase I and II metabolic enzymes, ultimately inducing systemic oxidative stress [20, 21]. Another study observed significant reductions in serum glycerophospholipid levels in mice after intratracheal instillation of PAHs, which promoted lung cancer progression [22]. Exposure to PAHs has also been shown to alter levels of triglycerides (TGs), phosphatidylcholines (PCs), phosphatidylethanolamines (PEs), and phosphatidylinositols (PIs), disrupting lipid metabolism, and leads to hepatocyte damage and systemic inflammation [23]. We therefore hypothesized that B[a]P could interfere with lipid homeostasis in dental epithelial tissues by modulating glycerophospholipid levels, with potential consequences for enamel formation.

Consequently, this study establishes a rat model of DDE induced by B[a]P exposure. Metabolic and transcriptomic profiles of dental epithelial cells from normal and DDE rats were constructed to investigate metabolic alterations during the development and progression of exposure-induced DDE, with a particular focus on glycerophospholipid levels. We hypothesize that B[a]P promotes the formation and development of DDE via enhancing glycerophospholipid biosynthesis in dental epithelial cells. The work aims to identify a potential approach for DDE prevention, providing further theoretical support for promoting early-life oral health management in children.

Materials and methods

Animals

All animal procedures and housing protocols were approved by the Ethics Committee of Peking University Health Science Center and conducted in accordance with ARRIVE guidelines (https://arriveguidelines.org). Sprague Dawley (SD) rats (Beijing Vital River Laboratory Animal Technology Co., Ltd.) were maintained in a specific pathogen–free facility under a 12-hour light/dark cycle with controlled temperature and humidity, with free access to food and water. Following mating, pregnant SD rats were randomly assigned to either a negative control group (NC) or a B[a]P-treatment group (BaP). Each group contained 9 dams, with 6 litters designated for metabolomic analysis and 3 litters for transcriptomic analysis. To simulate potential long-term environmental exposure during early life, offspring rats received daily administrations from postnatal day 1 to day 42. Because oral gavage is difficult in newborn rats and the efficiency of B[a]P transfer via breast milk are unclear, we selected intraperitoneal injection with a fine insulin syringe needle to achieve a more controllable B[a]P exposure, mimicking dietary exposure of man [24]. Rats in the BaP group were injected daily with 5 μg/kg of B[a]P (MedChemExpress), whereas rats in the NC group received an equal volume of physiological saline.

Mandible samples were collected from the euthanized animals on postnatal day 42. A bone window was created on the labial bone plate of the mandible overlying the labial cervical loop under a stereomicroscope. The surrounding mandibular tissue was then carefully dissected to expose the intact cervical loop structure. Following the protocol of Miquella [25], the mesenchymal and epithelial tissues were separated. Finally, the dental epithelial tissue, which contained dental epithelial stem cells (DESCs) and ameloblasts, was carefully collected with micro-forceps. The collected tissues were flash-frozen in liquid nitrogen and stored at -80 °C for later analysis.

Hematological parameters

Blood samples were collected and analyzed to determine lipid profiles and liver function, measuring TGs, cholesterol (CHO), high-density lipoprotein cholesterol

(HDL-C), low-density lipoprotein cholesterol (LDL-C), alanine transaminase (ALT), aspartate transaminase (AST), alkaline phosphatase (ALP), γ-glutamyltransferase (γ-GT), and total bilirubin (TBIL).

Cell isolation and culture

Six-week-old adult SD rats were euthanized via carbon dioxide overdose, and mandible samples were subsequently collected. The DESCs were then isolated and cultured according to the protocol established by Miquella [25]. Cells were exposed to BMP-4 (50 ng/ml, Peprotech), B[a]P (100 μM) and PC(P-16:0/0:0) (10 μM, MedChemExpress) in designated groups.

Micro CT

Rats were euthanized via carbon dioxide overdose, and their mandibles were collected and stored in PBS (Gibco). Mandibular incisors were then scanned using a VivaCT40 system (SCANO) at 75 kV and 6 W. The resulting micro-CT images were analyzed with ImageJ software to quantify enamel intensity.

RT-PCR

Total RNA was extracted using TRIzol reagent (Invitrogen) and reverse-transcribed into cDNA with HiScript III RT SuperMix for qPCR (+gDNA wiper; Vazyme). Real-time RT-PCR was performed on an ABI 7900 system (Applied Biosystems) with ChamQ Universal SYBR qPCR Master Mix (Vazyme). The primers used in this study are listed in Supplementary Table 1. Reactions were normalized to *β-actin*, and relative gene expression levels were analyzed via the ΔΔCt method.

RNA-sequencing

The RNA libraries were sequenced by OE Biotech, Inc., Shanghai, China. RNA purity and quantification were evaluated using the NanoDrop 2000 spectrophotometer (Thermo Scientific, USA). RNA integrity was assessed using the Agilent 2100 Bioanalyzer (Agilent Technologies, Santa Clara, CA, USA). Libraries were prepared with the VAHTS Universal V10 RNA-seq Library Prep Kit (Premixed Version) following the manufacturer's protocol. Sequencing was carried out on an Illumina Novaseq 6000 platform, yielding 150 bp paired-end reads. About 26 raw reads for each sample were generated. Raw reads of fastq format were firstly processed using fastp [26] and the low quality reads were removed to obtain the clean reads. Then about 24 clean reads for each sample were retained for subsequent analyses. The clean reads were mapped to the reference genome using HISAT2 [27]. FPKM [28] of each gene was calculated and the read counts of each gene were obtained by HTSeq-count [29]. PCA analysis were performed using R (v 3.2.0) to evaluate the biological duplication of samples. Differential expression analysis was performed using the DESeq2 [30]. Q value < 0.05 and foldchange > 2 or foldchange < 0.5 was set as the threshold for significantly differential expression gene (DEGs).

We performed hierarchical cluster analysis of these DEGs using R (v 3.2.0) to visualize their expression patterns across the different groups and samples. A radar chart of the top 30 genes was then generated with the R package ggradar to illustrate the expression levels of the most up- and down-regulated DEGs. Based on the hypergeometric distribution, GO [31], KEGG [32] pathway, Reactome and WikiPathways enrichment analysis of DEGs were performed to screen the significant enriched term using R (v 3.2.0), respectively. R (v 3.2.0) was used to draw the column diagram, the chord diagram and bubble diagram of the significant enrichment term. Sequencing read quality was assessed based on per base quality and per base sequence content. For the entire reference transcriptome project, a comprehensive evaluation was conducted using RseqQC [33] from three aspects: sequencing saturation, randomness of sequencing library construction, and enrichment of reads across different genomic elements.

Non-targeted metabolomics analysis

The dental epithelial tissues were harvested from the two groups of SD rats described previously. The non-targeted metabolomic sequencing and analysis were performed by Shanghai Lu-Ming Biotech Co. Ltd. The experimental phase involved analyzing and evaluating the preprocessing, derivatization, sample injection, and mass spectrometry system stability through the use of internal standards and quality control (QC) samples. Following data transfer, normalization, redundancy removal, and peak merging, a data matrix was generated. This matrix was imported into R for Principal Component Analysis (PCA) to assess overall sample distribution and the stability of the analytical process. Orthogonal Partial Least-Squares-Discriminant Analysis (OPLS-DA) and Partial Least Squares-Discriminant Analysis (PLS-DA) were then utilized to identify differentially abundant metabolites between groups. To evaluate model quality and prevent overfitting, we employed 7-fold cross-validation and 200 iterations of Response Permutation Testing (RPT). The overall contribution of each variable to group discrimination was ranked according to its Variable Importance of Projection (VIP) score, derived from the OPLS-DA model. A two-tailed Student's T-test was further used to verify whether the metabolites of difference between groups were significant. Differential metabolites were subsequently identified by applying thresholds of VIP > 1.0 and $p < 0.05$.

Quantification and statistical analysis

All experiments were performed in at least three independent replicates. Normality was verified using the Shapiro-Wilk test, and statistical significance was evaluated with Student's t-test or one-way ANOVA, followed by Tukey's post hoc test for multiple comparisons.

Results

B[a]P exposure lead to functional disorder of liver

To investigate the role of B[a]P in the occurrence and development of DDE, we established a rat model of B[a]P exposure (Fig. 1A). During the exposure, no significant differences were observed in mortality (Fig. 1B) or body weight (Fig. 1C) between the BaP group and the NC group. Blood was collected from the orbital venous plexus for lipid profile analysis and there were no obvious changes in the levels of TG, CHO, HDL-C, or LDL-C in BaP group and the NC group (Fig. 1D), which indicated that exposure to 5 μg/kg B[a]P did not induce dyslipidemia in rats. Further serum biochemical analysis revealed abnormal liver function in the experimental group. Specifically, increased levels of ALT, ALP, γ-GT, and TBIL were detected, while the level of AST was decreased (Fig. 1D). These findings suggested that the exposure of B[a]P was accompanied with impaired liver function which might lead to dysregulated hepatic lipid metabolism.

B[a]P exposure affects the formation of hard tissues of teeth

Mandibular bone samples from rats in each group were collected and subjected to micro-CT scanning for three-dimensional reconstruction and analysis. The BaP group observed that some rats developed pits on the lingual surface of the mandibular incisors, accompanied by pulp cavity exposure (Fig. 2A). No apparent differences were found in the crown-root lengths of the first and second molars between groups. However, the crown-root length and root length of the third molars were sharply shorter in the BaP group than it in the NC group (Fig. 2B). Additionally, the anatomical crown lengths of all molars were markedly reduced in BaP group (Fig. 2C-D). Furthermore, B[a]P exposure resulted in a clear decrease in alveolar bone height in the mandibular molar region, with furcation involvement particularly prominent in the first molars (Fig. 2E).

B[a]P exposure forms the phenotype of enamel dysplasia

Three-dimensional reconstruction and subsequent analysis were performed on the rat mandible models. The results revealed that, compared with the control group, the eruption length of the mandibular incisors in the exposed group showed no significant change; however, the length of enamel formation was shortened, and the enamel volume was significantly reduced (Fig. 3A). A plane perpendicular to the long axis of the mandible was defined at the mesial surface of the mandibular first molar and translated 2 mm toward the incisal direction to analyze the dental tissue structure at the cross-section. Compared with the control group, the exposed group exhibited a decrease in the thickness of the root canal wall and an increase in the pulp chamber area at the incisor cross-section (Fig. 3B). Calculation of dental tissue density based on Hounsfield unit (Hu) values indicated that the densities of both enamel and dentin at the incisor cross-section were lower in the exposed group than in the control group (Fig. 3B), suggesting impaired formation of dental hard tissues and abnormal enamel development in B[a]P-exposed rats, thereby confirming the successful establishment of the DDE model. Furthermore, rat DESCs were cultured ex vivo and induced toward ameloblastic differentiation with B[a]P exposure (Fig. 3C). RT-PCR results demonstrated that after B[a]P treatment, the expression levels of *ki67*, *Pcna*, and *Ccnb1* were increased, the expression of *Sox2* and *Oct3/4* was upregulated, while the expression levels of *Enam*, *Amelx*, and *Ambn* were significantly depressed (Fig. 3C). These findings suggest that ex vivo B[a]P exposure promotes the proliferation of DESCs, affects their differentiation ability, and inhibits ameloblastic differentiation, thereby playing a role in the development of DDE. However, the specific mechanisms and in vivo effects of B[a]P in this process remain unclear.

The course of DDE is accompanied by significant changes of glycerol-phospholipid metabolism

To further analyze the metabolic changes in dental epithelial cells during DDE occurrence, dental epithelial cells from the cervical loop region of the mandibular incisors of DDE model and control group rats were collected for non-targeted metabolomic analysis using dual platforms. Both PCA and OPLS-DA indicated a significant difference in metabolite composition between the control and DDE groups (Fig. 4A). Screening for differential metabolites revealed that, compared to the control group, the levels of 496 metabolites were increased and the levels of 186 metabolites were decreased in the dental epithelial cells of the DDE rat group (Fig. 4B). Further filtering of the identified compounds was performed based on the confidence level of compound identification; metabolites rated at Level 1 and Level 2 were selected for subsequent validation. The number of carbon-carbon double bonds and carbon-carbon triple bonds was recorded based on the structural formulas of the metabolites. The results showed no statistically significant difference in the average number of carbon-carbon unsaturated bonds among the differential metabolites (Fig. 4C). However, further calculation of the unsaturation index (Fig. 4D) for the

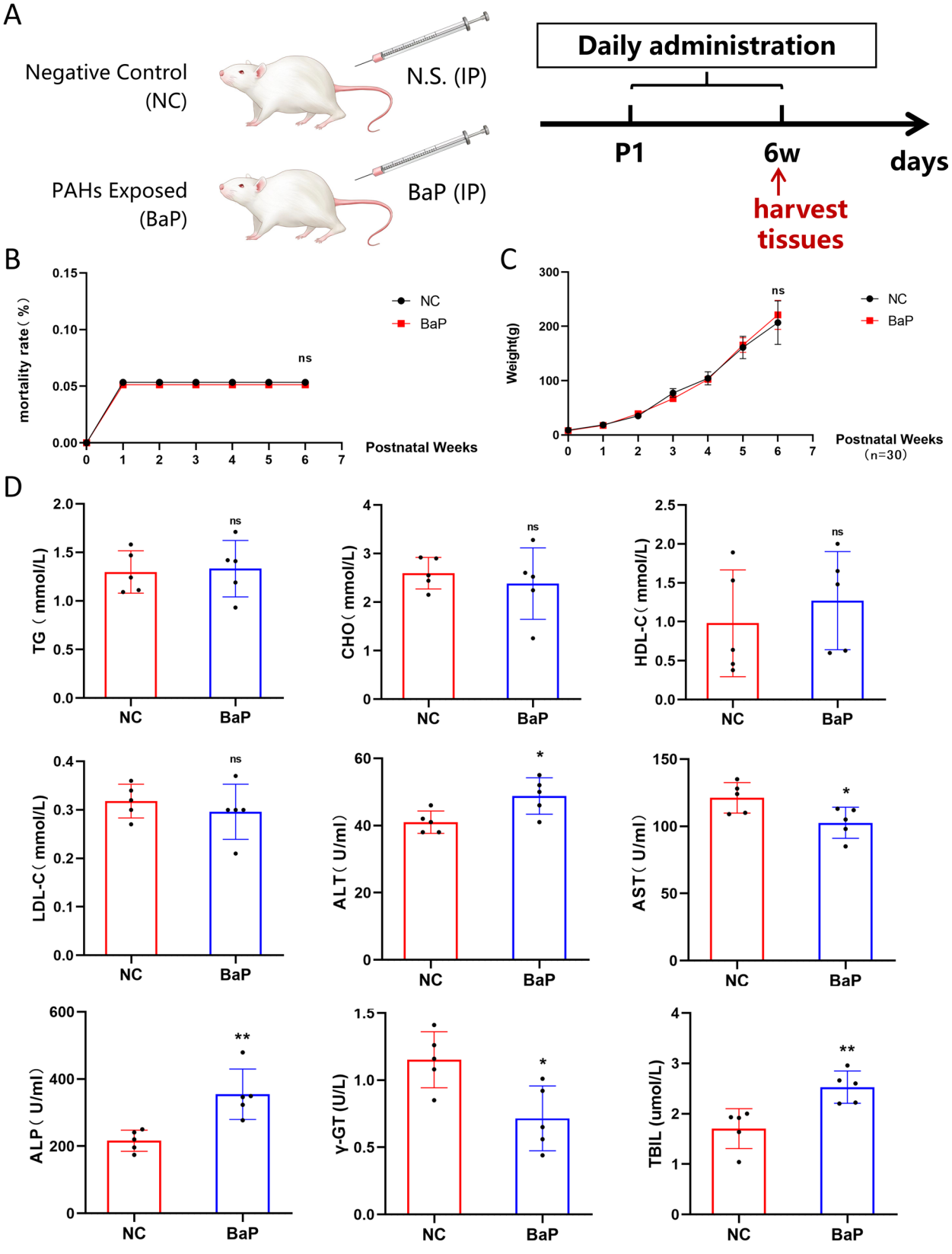

Fig. 1 B[a]P exposure affects liver function in rats. **A**: PAHs exposure model established by intraperitoneal injection of B[a]P; **B**: Mortality rate of rats; **C**: Body weight changes of rats; **D**: Hematological detection of rats. (*$P < 0.05$, **$P < 0.01$)

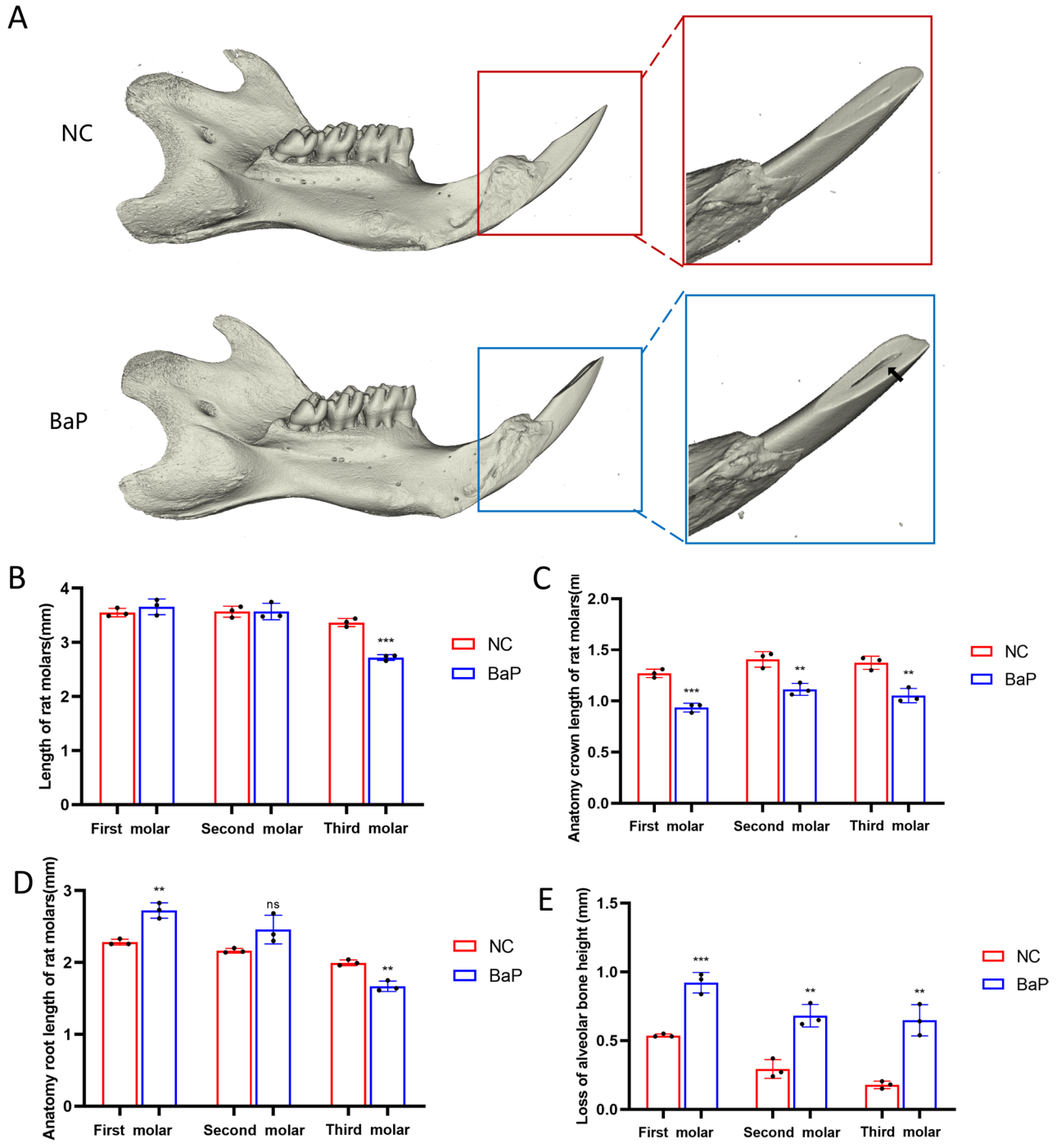

Fig. 2 B[a]P exposure affects crown and root development of incisors and molars. **A**: Three-dimensional reconstruction models of the mandibles (the arrow indicates the lingual depression of the mandibular incisor); **B–E**: Changes in dental hard tissues following B[a]P exposure measured base on 3D reconstruction models. (*$P < 0.05$, **$P < 0.01$, ***$P < 0.001$)

differential metabolites with increased and decreased levels revealed that the average unsaturation index of the metabolites with increased levels in the dental epithelial cells of the DDE group was significantly higher compared to that of the metabolites with decreased levels (Fig. 4E). KEGG pathway analysis indicated that the metabolites with increased levels were enriched in lipid metabolic pathways, including arachidonic acid metabolism, glycerophospholipid metabolism, and sphingolipid metabolism (Fig. 4F).

To elucidate the specific changes in metabolite abundance during the development of DDE, further

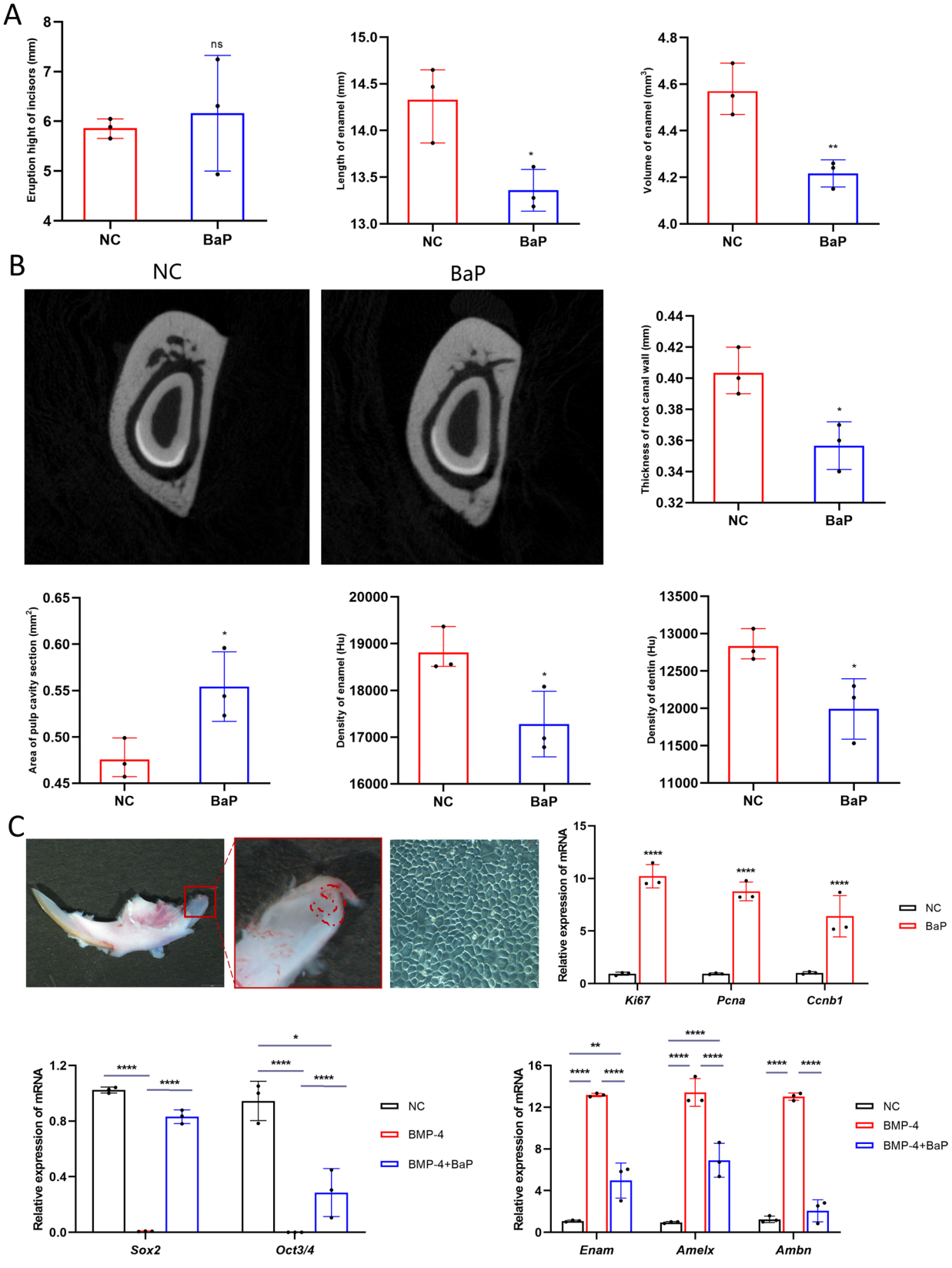

Fig. 3 B[a]P exposure leads to abnormal development of incisor enamel. **A**: Changes in incisor enamel length and volume; **B**: Cross-sectional analysis of rat mandibular incisor; **C**: In vitro culture of DESCs with B[a]P exposed, and detect the expression levels of related genes by qPCR. (*$P < 0.05$, **$P < 0.01$, ***$P < 0.001$, ****$P < 0.0001$)

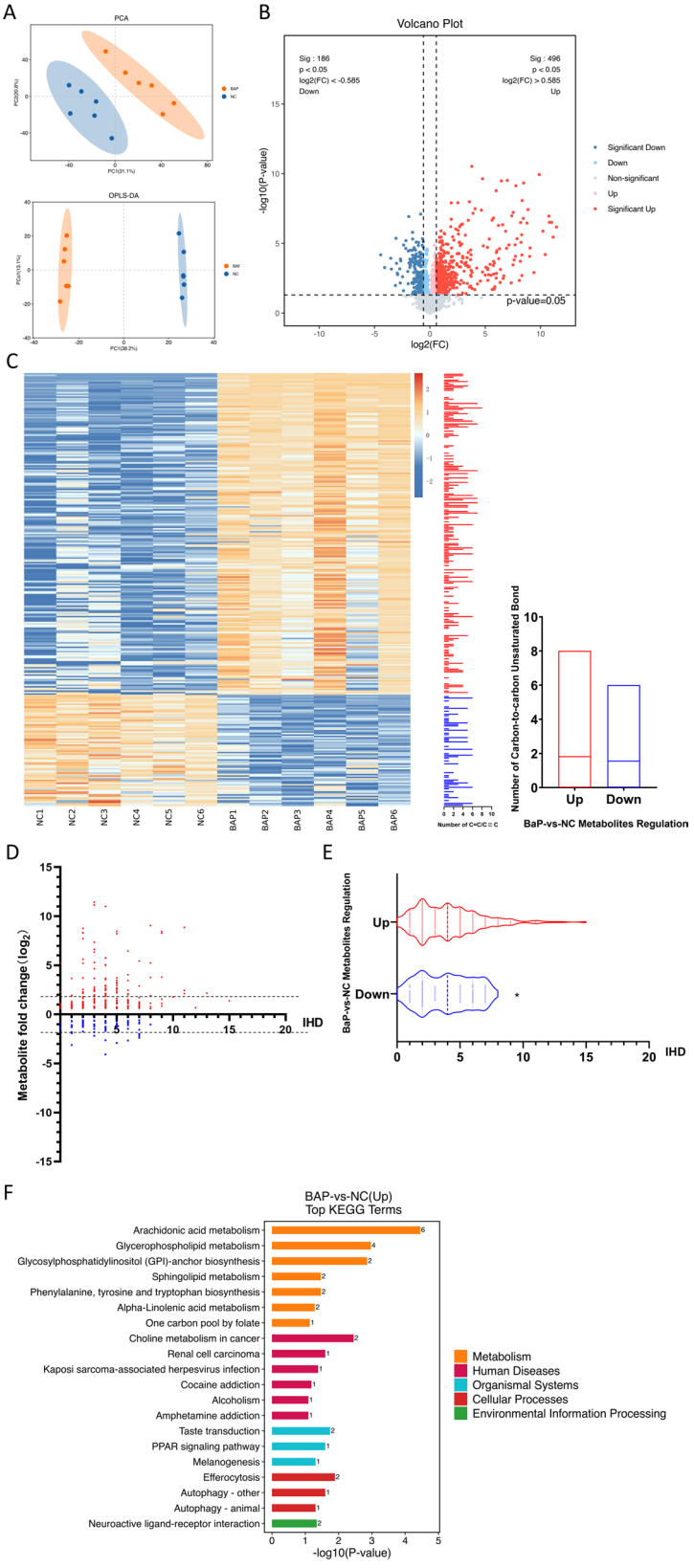

Fig. 4 Non-targeted metabolomic analysis using dual platforms on dental epithelial cells from DDE model rats. **A**: Metabolite composition analysis; **B**: Volcano plot of differential metabolites; **C**: Analysis of the number of carbon-carbon unsaturated bonds in differential metabolites; **D**, **E**: Analysis of unsaturation degree of differential metabolites; **F**: KEGG pathway analysis of differential metabolites. (*$P < 0.05$)

metabolite analysis was conducted on the two most significantly altered pathways, arachidonic acid metabolism and glycerophospholipid metabolism. KEGG pathway maps for these two metabolic pathways were generated. In the arachidonic acid metabolism pathway, the levels of 5 S-HETE (Fig. 5A), 12-keto-10,11,14,15-tetrahydro-LTB4 (Fig. 5C), 15 S-HETE (Fig. 5D), Trioxilin A3 (Fig. 5E), Troxilin B3 (Fig. 5F), and various glycerophospholipids (Fig. 5B) were increased. In the glycerophospholipid metabolism pathway, only the level of phosphorylcholine (Fig. 6E) was decreased, while the other enriched metabolites were also glycerophospholipids (Fig. 6A-D). These results indicate that among the metabolic pathways with increased abundance, the major altered metabolites were glycerophospholipids, revealing that BaP exposure can lead to active glycerophospholipid

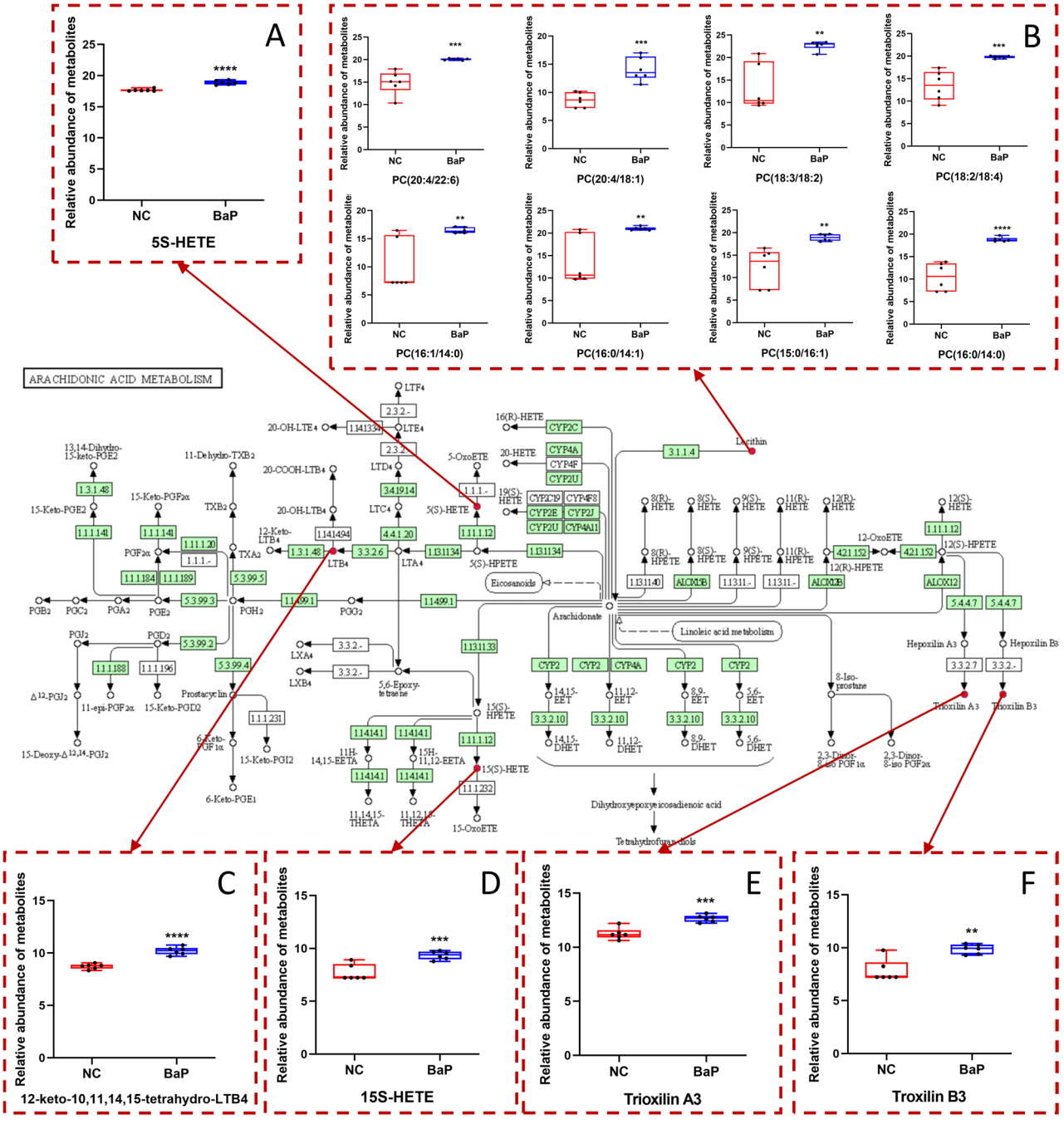

Fig. 5 Changes in metabolite abundance in the arachidonic acid metabolism pathway. **A**: Changes of 5 S-HETE; **B**: Changes of glycerophospholipids; **C**: Changes of 12-keto-10,11,14,15-tetrahydro-LTB4; **D**: Changes of 15 S-HETE; **E**: Changes of Trioxilin A3; **F**: Changes of Troxilin B3. (**$P < 0.01$, ***$P < 0.001$, ****$P < 0.0001$)

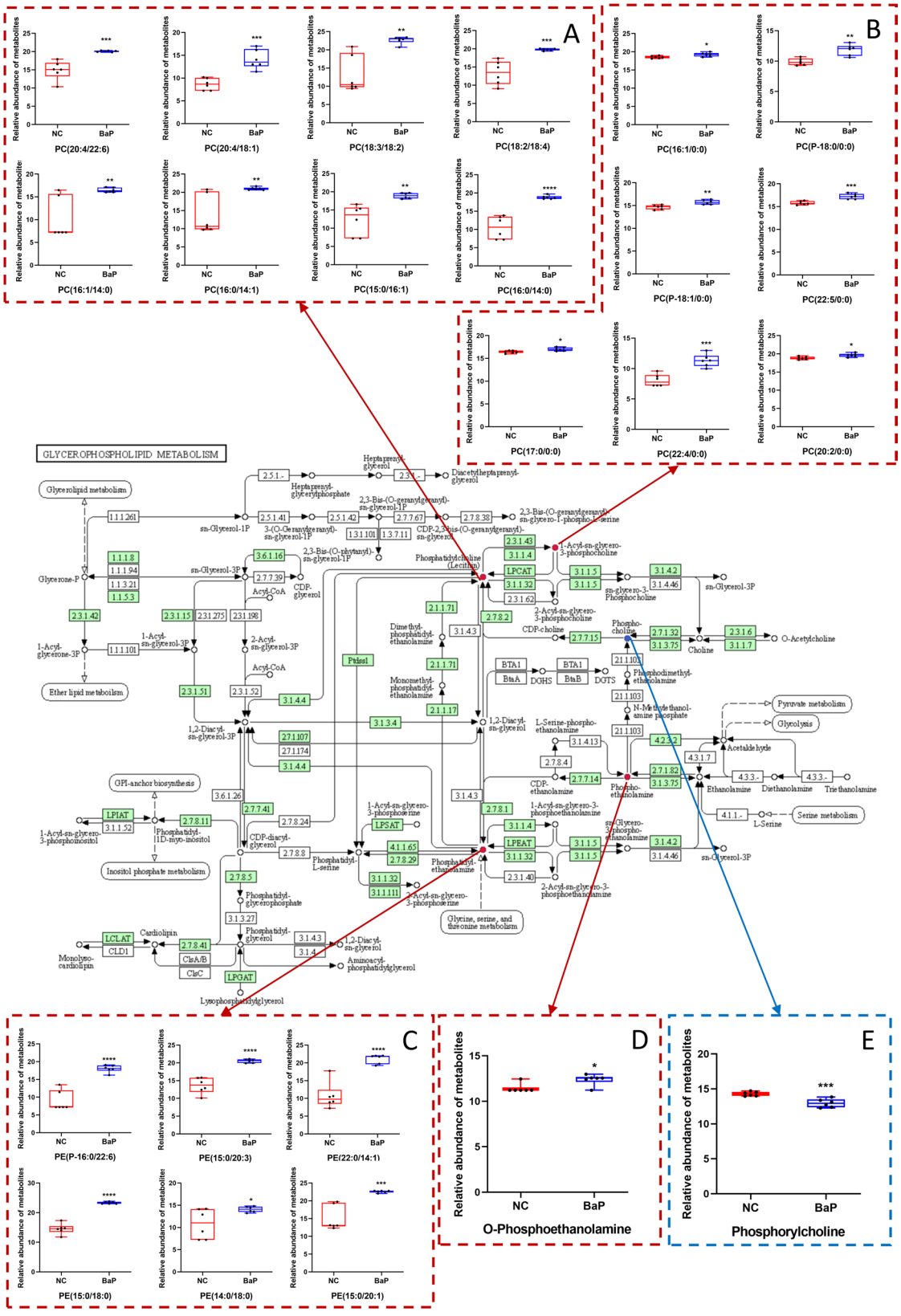

Fig. 6 Changes in metabolite abundance in the glycerophospholipid metabolism pathway. **A**–**C**: Changes of glycerophospholipids; **D**: Changes of O-Phosphoethanolamine; **E**: Changes of phosphorylcholine. (*$P < 0.05$, **$P < 0.01$, ***$P < 0.001$, ****$P < 0.0001$)

metabolism and elevated glycerophospholipid levels in dental epithelial tissues. This further confirms the close relationship between glycerophospholipid metabolism and the development of DDE induced by environmental exposure.

Genes involved in glycerophospholipid synthesis and hydrolysis are the potential targets for rescuing the DDE phenotype

To identify key genes that play a regulatory role in the pathophysiology of DDE, this study screened differentially expressed genes involved in glycerophospholipid metabolic pathways. During the development of DDE, 778 differentially expressed genes were found to be upregulated, while 89 were downregulated in the dental epithelium (Fig. 7A). Among these, the expression levels of ameloblast differentiation-related genes, including *Enam*, *Amelx*, *Ambn*, and *Mmp20*, were significantly downregulated (Fig. 7B), which further confirmed the successful establishment of a rat DDE model through B[a]P exposure. Integrated transcriptomic and metabolomic analysis revealed a significant positive correlation between the transcriptional levels of ameloblast differentiation-related genes and the content of glycerophospholipids (Fig. 7C). Differentially expressed genes involved in the glycerophospholipid metabolism pathway were screened for subsequent analysis (Fig. 7D).

The metabolite PC(P-16:0/0:0), previously shown to be significantly up-regulated during DDE pathogenesis in metabolomic studies, was administered ex vivo cell culture. Its effects on the ameloblastic differentiation of dental epithelial cells were then assessed. The results showed that PC(P-16:0/0:0) down-regulated the expression of *Amelx* and *Ambn* in dental epithelial cells (Fig. 7E), thereby inhibiting the ameloblastic differentiation. Concurrently, stimulation with PC(P-16:0/0:0) led to increased transcriptional levels of *Dgki* and *Dgkk* and decreased transcriptional levels of *Pla2g2a* and *Pla2g2c* in dental epithelial cells (Fig. 7E). Together, these genes regulate glycerophospholipid metabolic homeostasis in dental epithelial cells, affect cell fate determination, and interfere with enamel formation.

Discussion

Enamel formation is a complex and orderly physiological process involving numerous cells and their molecular interactions. Any abnormality in a single factor may lead to enamel formation defects. The metabolome serves as a critical bridge between environmental factors and development, significantly expanding our understanding of abnormal enamel development. In this study, a rat model of DDE was established. Specific alterations in the metabolome of rat DECs were identified before and after DDE formation, confirming that abnormal phospholipid metabolism accompanies the development of DDE. Furthermore, potential targets for rescuing DDE were untangled.

Previous studies have indicated that early-life exposure to environmental endocrine disruptors is closely associated with enamel development and the onset and progression of DDE. Some researchers have demonstrated that exposure to the environmental stimulant bisphenol A can lead to developmental defects in the incisor enamel of mice, resulting in impaired enamel formation [6]. Additionally, studies using a prenatal nicotine exposure mouse model have revealed that early-life nicotine exposure can interfere with enamel formation in mice, leading to hypomineralization manifestations such as white opaque alterations and microstructural disorganization in the enamel [7]. Our research set up a DDE model by B[a]P exposure via intraperitoneal injection. This model also revealed that B[a]P exposure adversely affects crown and root development in both incisors and molars, exacerbates alveolar bone loss, and plays an important role in the formation of dental hard tissues. Besides, those pits observed in BaP group may be attributed to reduced density of dental hard tissues following B[a]P exposure, leading to accelerated incisal wear.

Previous studies have found that PAHs exposure in mice leads to altered levels of lipid metabolites in the liver, disrupts the metabolism of glycerolipids, glycerophospholipids, and fatty acids, and subsequently causes hepatocyte damage, inflammation, and other systemic abnormalities [22]. Another study, by evaluating the lipid metabolic response of mice to intratracheally administered PAHs, revealed that airway PAHs exposure significantly reduced serum levels of glycerophospholipids promoting the progression of lung cancer [23]. In our study, it was confirmed that the exposure of B[a]P was accompanied with impaired liver function in rat which might lead to dysregulated hepatic lipid metabolism.

Lipid metabolism, particularly fatty acid oxidation, is conventionally regarded as a major source of cellular energy. However, recent studies have revealed its close association with cell fate determination. The concept that lipid accumulation in tissues leads to cellular dysfunction has gained increasing acceptance [34]. The mechanisms by which lipid overload induces cellular damage or lipotoxicity have been extensively investigated in tissues such as the kidney, liver, heart, skeletal muscle, bone, pancreas, and brain [35]. Furthermore, inhibition of lipid metabolism has been shown to suppress oocyte differentiation and impair embryonic development [36]. Our screening revealed that DDE formation is also closely associated with the lipid metabolim. The occurrence of DDE was accompanied by significant enrichment of glycerophospholipid metabolites, and the related transcription factors *Dgki* and *Dgkk*, along with *Pla2g2a* and *Pla2g2c*,

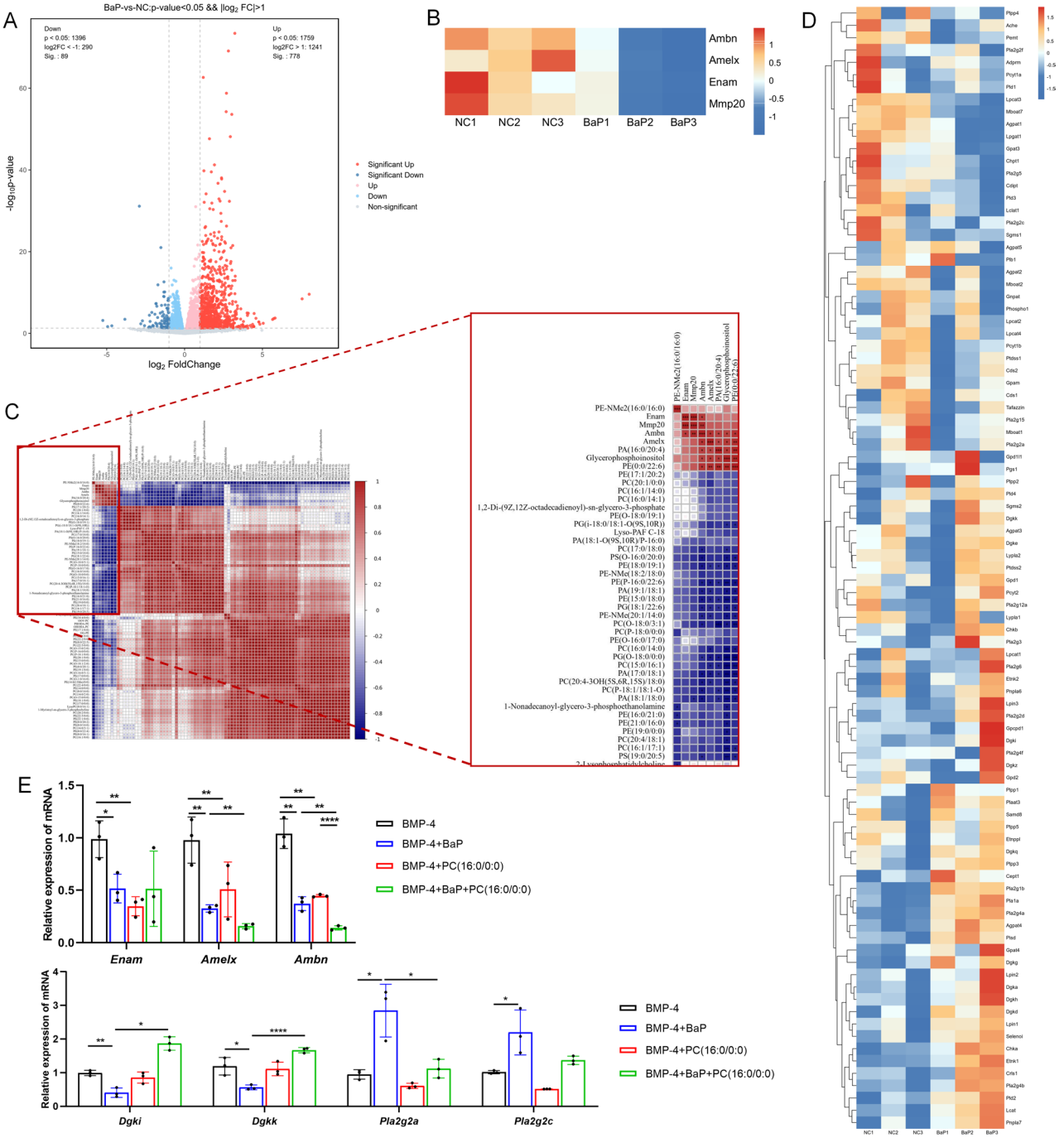

Fig. 7 Regulatory role of glycerophospholipid metabolism in dental epithelium during DDE formation. **A**: Volcano plot of differential genes; **B**: Changes of ameloblast differentiation-related genes; **C**: Metabolomic and transcriptomic combined analysis; **D**: Transcriptional changes in glycerophospholipid metabolism pathway; **E**: In vitro culture of DESCs with B[a]P exposed and glycerophospholipid rescued, and detect the expression levels of related genes by qPCR. (*$P < 0.05$, **$P < 0.01$, ****$P < 0.0001$)

were implicated in regulating the ameloblastic differentiation of DESCs. *Dgki* and *Dgkk* are genes involved in glycerophospholipid synthesis and regulate intracellular glycerophospholipid concentrations through the phosphorylation of diacylglycerol [37]. In contrast, the proteins encoded by *Pla2g2a* and *Pla2g2c* belong to the phospholipase A2 family, which catalyzes the hydrolysis of the sn-2 acyl ester bond in phosphoglycerides, releasing free fatty acids and lysophospholipids, and participates in regulating glycerophospholipid metabolism in cellular biomembranes [38, 39]. Thus, our findings indicate that increasing glycerophospholipid synthesis while

inhibiting phospholipid hydrolysis in DESCs exacerbates the inhibition of B[a]P on their ameloblastic differentiation capacity. This further confirms that lipid metabolism regulates the differentiation potential of DESCs and enamel development.

The prenatal and perinatal periods represent a unique physiological phase characterized by diverse environmental stimuli and complex pathways influencing growth and development. Metabolomics can more directly reflect physiological changes within the body and provide better insights into biomolecular functions and regulatory mechanisms [40]. For instance, to explore the mechanisms and metabolic biomarkers of adverse pregnancy outcomes induced by mono (2-ethylhexyl) phthalate (MEHP) exposure, one study employed metabolomics to determine the metabolic profiles of HTR-8/Svneo cells exposed to different doses of MEHP, established a dose–response relationship between MEHP exposure and metabolic alterations in trophoblasts, and identified sensitive endogenous biomarkers of MEHP exposure [41]. Another study exposed mice to filtered air or concentrated ambient $PM_{2.5}$ during the pre-pregnancy and gestational periods, and used metabolomics to analyze maternal serum and placental metabolic profiles, revealing the impact of $PM_{2.5}$ exposure on placental nutrient transport capacity [42]. In the present study, comparative analysis of differential metabolites in dental epithelial cells between DDE model and control rats showed that glycerophospholipid metabolites comprised the majority of altered compounds among the upregulated metabolic pathways in the DDE group, further supporting a close association between glycerophospholipid metabolism and DDE development. The specific regulatory role, however, remains to be elucidated.

In summary, this study established a rat DDE model via B[a]P exposure, constructed metabolic and transcriptomic profiles of dental epithelial cells in both normal and DDE rats, explored metabolic alterations in dental epithelial cells after B[a]P exposure, and preliminarily investigated the mechanism by which B[a]P-induced phospholipid metabolic disorders affect enamel formation. However, due to differences between tooth development in human and the continuously growing incisor in rats, the applicability of these results to humans is limited. Furthermore, B[a]P exposure occurs via inhalation and oral intake, and the total exposure dose during maternal pregnancy and early childhood is difficult to quantify. Therefore, the dose of B[a]P exposure used in this study and the rescue effects of glycerophospholipid observed at this dose serve only as a laboratory reference. More in-depth research is required in the future to explore strategies applicable for rescuing human DDE caused by B[a]P exposure.

Conclusion

This study established a rat model of DDE and confirmed that B[a]P exposure exerts multifaceted impacts on tooth development, revealing a correlation between altered phospholipid metabolism and transcriptional changes in enamel formation-related genes. These findings prove an association between environmental factors and DDE and suggest potential strategies for its prevention, thereby providing further theoretical support for early childhood oral health management. Further mechanistic and translational research is required to validate the applicability of this pathway in human populations.

Abbreviations

DDE	Developmental defects of enamel
B[a]P	Benzo[a]pyrene
MIH	Molar-incisor hypomineralisation
EEDs	Environmental endocrine disruptors
PAHs	Polycyclic aromatic hydrocarbons
TG	Triglycerides
CHO	Cholesterol
HDL-C	High-density lipoprotein cholesterol
LDL-C	Low-density lipoprotein cholesterol
ALT	Alanine transaminase/glutamic-pyruvic transaminase
AST	Aspartate transaminase/glutamic-oxaloacetic transaminase
ALP	Alkaline phosphatase
γ-GT	γ-glutamyltransferase
TBIL	Total bilirubin
DESCs	Dental epithelial stem cells
DECs	Dental epithelial cells

Supplementary Information

The online version contains supplementary material available at https://doi.org/10.1186/s12903-026-08431-2.

Supplementary Material 1.

Acknowledgements

Not applicable.

Authors' contributions

YP and XW were involved in study conception and design. YP was chief performers of the study and were engaged in data analyses and interpretation. XF and YZ participated in in-vitro experiments. SY was involved in micro CT analysis and the design of graphical abstract. DC and XW provided valuable suggestions and comments. YP wrote the main manuscript text. All authors reviewed the manuscript.

Funding

This work was supported by Clinical Key Specialty Program from Peking University School and Hospital of Stomatology (PKUSSNKP-202107) Xiaoyan Wang in the design of the study and collection, analysis of data, and by the Shandong Provincial Natural Science Foundation (ZR2024QH484) and the Qingdao Natural Science Foundation (24-4-4-zrjj-120-jch) Dixin Cui in the interpretation of data and in writing the manuscript.

Data availability

Raw data were generated at Department of Cariology and Endodontology, Peking University and Hospital of Stomatology. The raw RNA sequence data reported in this paper have been deposited in the Genome Sequence Archive (Genomics, Proteomics & Bioinformatics 2025) in National Genomics Data Center (Nucleic Acids Res 2025), China National Center for Bioinformation / Beijing Institute of Genomics, Chinese Academy of Sciences (GSA: CRA041075) that are publicly accessible at https://ngdc.cncb.ac.cn/gsa [43, 44]. Other

derived data supporting the findings of this study are available from the author, Yue Pan, on request.

Declarations

Ethics approval and consent to participate

All experiments involved with animals were followed the guidelines approved by State Key Laboratory of Oral Diseases and were in accordance with ARRIVE guidelines (https://arriveguidelines.org). The study was granted by the Ethics Committee of Peking University Health Science Center (PUIRB-LA2024093, Mar.04, 2024).

Consent for publication

Not applicable.

Competing interests

The authors declare no competing interests.

Author details

[1]Department of Cariology and Endodontology, Peking University School and Hospital of Stomatology & National Clinical Research Center for Oral Diseases & National Engineering Research Center of Oral Biomaterials and Digital Medical Devices, Beijing, China
[2]Department of Pediatric Dentistry, West China School of Stomatology, Sichuan University, Chengdu, China
[3]Department of Pediactric Dentistry, Qingdao Stomatological Hospital Affiliated to Qingdao University, Qingdao, China

Received: 19 February 2026 / Accepted: 20 April 2026
Published online: 27 April 2026

References

1. DeRocher KA, Smeets PJM, Goodge BH, Zachman MJ, Balachandran PV, Stegbauer L, Cohen MJ, Gordon LM, Rondinelli JM, Kourkoutis LF, Joester D. Chemical gradients in human enamel crystallites. Nature. 2020;583(7814):66–71. https://doi.org/10.1038/s41586-020-2433-3. Epub 2020 Jul 1. Erratum in: Nature. 2020;584(7819):E3. https://doi.org/10.1038/s41586-020-2544-x. PMID: 32612224; PMCID: PMC8290891.
2. Winkler JR, Dixon BL, Singh I, Soto R, Qiu Y, Zhang Y, Porucznik CA, Stanford JB. Prenatal exposure to environmental toxins and comprehensive dental findings in a population cohort of children. BMC Oral Health. 2024;24(1):326. https://doi.org/10.1186/s12903-023-03786-2. PMID: 38468230; PMCID: PMC10929125.
3. Sluka B, Held U, Wegehaupt F, Neuhaus KW, Attin T, Sahrmann P. Is there a rise of prevalence for Molar Incisor Hypomineralization? A meta-analysis of published data. BMC Oral Health. 2024;24(1):127. https://doi.org/10.1186/s12903-023-03637-0. PMID: 38273324; PMCID: PMC10809700.
4. Perera F, Herbstman J. Prenatal environmental exposures, epigenetics, and disease. Reprod Toxicol. 2011;31(3):363–73.
5. Chen G, Chen J, Yan Z, et al. Maternal diabetes modulates dental epithelial stem cells proliferation and self-renewal in offspring through apurinic/apyrimidinicendonuclease1-mediated DNA methylation. Sci Rep. 2017;7:40762.
6. Li H, Cui D, Zheng L, Zhou Y, Gan L, Liu Y, Pan Y, Zhou X, Wan M. Bisphenol A Exposure Disrupts Enamel Formation via EZH2-Mediated H3K27me3. J Dent Res. 2021;100(8):847–857. https://doi.org/10.1177/0022034521995798. Epub 2021 Mar 3. PMID: 33655795.
7. Tian QL, Zhao DF, Guan SY, Zhou Y, Zhou X, Zheng LW. [Effects of prenatal nicotine exposure on enamel formation of offspring mice]. Zhonghua Kou Qiang Yi Xue Za Zhi. 2023;58(1):40–49. Chinese. https://doi.org/10.3760/cma.j.cn112144-20220922-00499. PMID: 36642451.
8. Zhang Y, Yang Y, Chen W, Mi C, Xu X, Shen Y, Zheng Z, Xu Z, Zhao J, Wan S, Wang X, Zhang H. BaP/BPDE suppressed endothelial cell angiogenesis to induce miscarriage by promoting MARCHF1/GPX4-mediated ferroptosis. Environ Int. 2023;180:108237. https://doi.org/10.1016/j.envint.2023.108237. Epub 2023 Sep 28. PMID: 37802009.
9. Yang Q, Qiu X, Li R, Ma J, Li K, Li G. Polycyclic aromatic hydrocarbon (PAH) exposure and oxidative stress for a rural population from the North China Plain. Environ Sci Pollut Res Int. 2015;22(3):1760-9. https://doi.org/10.1007/s11356-014-3284-y. PMID: 25015715.
10. Ramesh A, Walker SA, Hood DB, et al. Bioavailability and risk assessment of orally ingested polycyclic aromatic hydrocarbons. Int J Toxicol. 2004;23:301–33.
11. Ifegwu C, Osunjaye K, Fashogbon F, Oke K, Adeniyi A, Anyakora C. Urinary 1-hydroxypyrene as a biomarker to carcinogenic polycyclic aromatic hydrocarbon exposure. Biomark Cancer. 2012;4:7–17. https://doi.org/10.4137/BIC.S10065. PMID: 24179391; PMCID: PMC3791913.
12. Simko PP. Determination of polycyclic aromatic hydrocarbons in smoked meat products and smoke flavouring food additives. Chromatogr J. 2002;770:3–18.
13. Ifegwu OC, Anyakora C. Polycyclic Aromatic Hydrocarbons: Part I. Exposure. Adv Clin Chem. 2015;72:277–304. https://doi.org/10.1016/bs.acc.2015.08.001. Epub 2015 Sep 26. PMID: 26471085.
14. IARC Working Group on the Evaluation of Carcinogenic Risks to Humans. Some non-heterocyclic polycyclic aromatic hydrocarbons and some related exposures. IARC Monogr Eval Carcinog Risks Hum. 2010;92:1–853. PMID: 21141735; PMCID: PMC4781319.
15. Lackmann GM, Göen T, Töllner U, et al. PCBs and HCB in serum of full-term German neonates. Lancet. 1996;348:1035.
16. Alaluusua S, Lukinmaa PL. Developmental dental toxicity of dioxin and related compounds–a review. Int Dent J. 2006;56(6):323 – 31. https://doi.org/10.1111/j.1875-595x.2006.tb00336.x. PMID: 17243464.
17. Peltonen E, Lukinmaa P-L, Sahlberg C, et al. 7,12-Dimethylbenz[a]anthracene interferes with the development of cultured mouse mandibular molars. Toxicol Sci. 2006;92:279–85.
18. Gao P, da Silva E, Hou L, Denslow ND, Xiang P, Ma LQ. Human exposure to polycyclic aromatic hydrocarbons: Metabolomics perspective. Environ Int. 2018;119:466–77. https://doi.org/10.1016/j.envint.2018.07.017. Epub 2018 Jul 20. PMID: 30032012.
19. Wang Z, Zheng Y, Zhao B, Zhang Y, Liu Z, Xu J, Chen Y, Yang Z, Wang F, Wang H, He J, Zhang R, Abliz Z. Human metabolic responses to chronic environmental polycyclic aromatic hydrocarbon exposure by a metabolomic approach. J Proteome Res. 2015;14(6):2583–93. https://doi.org/10.1021/acs.jproteome.5b00134. Epub 2015 May 27. PMID: 25990285.
20. Dalton TP, Puga A, Shertzer HG. Induction of cellular oxidative stress by aryl hydrocarbon receptor activation. Chem Biol Interact. 2002;141(1–2):77–95. https://doi.org/10.1016/s0009-2797(02)00067-4. PMID: 12213386.
21. Moorthy B, Chu C, Carlin DJ. Polycyclic aromatic hydrocarbons: from metabolism to lung cancer. Toxicol Sci. 2015;145(1):5–15. https://doi.org/10.1093/toxsci/kfv040. PMID: 25911656; PMCID: PMC4408964.
22. Li F, Xiang B, Jin Y, Li C, Li J, Ren S, Huang H, Luo Q. Dysregulation of lipid metabolism induced by airway exposure to polycyclic aromatic hydrocarbons in C57BL/6 mice. Environ Pollut. 2019;245:986–93. https://doi.org/10.1016/j.envpol.2018.11.049. Epub 2018 Nov 21. PMID: 30682755.
23. Li F, Xiang B, Jin Y, Li C, Ren S, Wu Y, Li J, Luo Q. Hepatotoxic effects of inhalation exposure to polycyclic aromatic hydrocarbons on lipid metabolism of C57BL/6 mice. Environ Int. 2020;134:105000. https://doi.org/10.1016/j.envint.2019.105000. Epub 2019 Nov 4. PMID: 31699440.
24. Foth H, Kahl R, Kahl GF. Pharmacokinetics of low doses of benzo[a]pyrene in the rat. Food Chem Toxicol. 1988;26(1):45–51. https://doi.org/10.1016/0278-6915(88)90040-3. PMID: 3345969.
25. Chavez MG, Hu J, Seidel K, Li C, Jheon A, Naveau A, Horst O, Klein OD. Isolation and culture of dental epithelial stem cells from the adult mouse incisor. J Vis Exp. 2014;8751266. https://doi.org/10.3791/51266. PMID: 24834972; PMCID: PMC4141628.
26. Chen S, Zhou Y, Chen Y, Gu J. fastp: an ultra-fast all-in-one FASTQ preprocessor. Bioinformatics. 2018;34(17):i884–90. https://doi.org/10.1093/bioinformatics/bty560. PMID: 30423086; PMCID: PMC6129281.
27. Kim D, Langmead B, Salzberg SL. HISAT: a fast spliced aligner with low memory requirements. Nat Methods. 2015;12(4):357–60. https://doi.org/10.1038/nmeth.3317. Epub 2015 Mar 9. PMID: 25751142; PMCID: PMC4655817.
28. Roberts A, Trapnell C, Donaghey J, Rinn JL, Pachter L. Improving RNA-Seq expression estimates by correcting for fragment bias. Genome Biol. 2011;12(3):R22. https://doi.org/10.1186/gb-2011-12-3-r22. Epub 2011 Mar 16. PMID: 21410973; PMCID: PMC3129672.
29. Anders S, Pyl PT, Huber W. HTSeq–a Python framework to work with high-throughput sequencing data. Bioinformatics. 2015;31(2):166–9. https://doi.org/10.1093/bioinformatics/btu638. Epub 2014 Sep 25. PMID: 25260700; PMCID: PMC4287950.
30. Love MI, Huber W, Anders S. Moderated estimation of fold change and dispersion for RNA-seq data with DESeq2. Genome Biol. 2014;15(12):550. https://doi.org/10.1186/s13059-014-0550-8. PMID: 25516281; PMCID: PMC4302049.

31. The Gene Ontology Consortium. The Gene Ontology Resource: 20 years and still GOing strong. Nucleic Acids Res. 2019;47(D1):D330–8. https://doi.org/10.1093/nar/gky1055. PMID: 30395331; PMCID: PMC6323945.
32. Kanehisa M, Araki M, Goto S, Hattori M, Hirakawa M, Itoh M, Katayama T, Kawashima S, Okuda S, Tokimatsu T, Yamanishi Y. KEGG for linking genomes to life and the environment. Nucleic Acids Res. 2008;36(Database issue):D480-4. https://doi.org/10.1093/nar/gkm882. Epub 2007 Dec 12. PMID: 18077471; PMCID: PMC2238879.
33. Wang L, Wang S, Li W, et al. RSeQC: Quality Control of RNA-seq experiments[J]. Bioinformatics. 2012;28(16):2184–5.
34. Xiong J. Fatty Acid Oxidation in Cell Fate Determination. Trends Biochem Sci. 2018;43(11):854–7.
35. Yoon H, Shaw JL, Haigis MC, Greka A. Lipid metabolism in sickness and in health: Emerging regulators of lipotoxicity. Mol Cell. 2021;81(18):3708–30. https://doi.org/10.1016/j.molcel.2021.08.027. PMID: 34547235; PMCID: PMC8620413.
36. Dunning KR, Cashman K, Russell DL, Thompson JG, Norman RJ, Robker RL. Beta-oxidation is essential for mouse oocyte developmental competence and early embryo development. Biol Reprod. 2010;83(6):909–18.
37. Liu Y, Yang Z, Zhou X, Li Z, Hideki N. Diacylglycerol Kinases and Its Role in Lipid Metabolism and Related Diseases. Int J Mol Sci. 2024;25(23):13207. https://doi.org/10.3390/ijms252313207. PMID: 39684917; PMCID: PMC11643042.
38. Tremblay BL, Cormier H, Rudkowska I, Lemieux S, Couture P, Vohl MC. Association between polymorphisms in phospholipase A2 genes and the plasma triglyceride response to an n-3 PUFA supplementation: a clinical trial. Lipids Health Dis. 2015;14:12. https://doi.org/10.1186/s12944-015-0009-2. PMID: 25889305; PMCID: PMC4342012.
39. Gao Y, Yang Z, Bajpai AK, Wang W, Zhang L, Xia Z. Resveratrol enhances the antiliver cancer effect of cisplatin by targeting the cell membrane protein PLA2. Front Oncol. 2024;14:1453164. https://doi.org/10.3389/fonc.2024.1453164. PMID: 39381045; PMCID: PMC11458693.
40. Kwon YK, Lu W, Melamud E, et al. A domino effect in antifolate drug action in Escherichia coli[J]. Nat Chem Biol. 2008;4(10):602–8.
41. Fang Y, Chen Z, Chen J, Zhou M, Chen Y, Cao R, Liu C, Zhao K, Wang M, Zhang H. Dose-response mapping of MEHP exposure with metabolic changes of trophoblast cell and determination of sensitive markers. Sci Total Environ. 2023;855:158924.
42. Tao S, Yang M, Pan B, Wang Y, Tian F, Han D, Shao W, Yang W, Xie Y, Fang X, Xia M, Hu J, Kan H, Li W, Xu Y. Maternal exposure to ambient PM2.5 perturbs the metabolic homeostasis of maternal serum and placenta in mice. Environ Res. 2023;216(Pt 3):114648.
43. Zhang S, Chen X, Jin E, Wang A, Chen T, Zhang X, Zhu J, Dong L, Sun Y, Yu C, Zhou Y, Fan Z, Chen H, Zhai S, Sun Y, Chen Q, Xiao J, Song S, Zhang Z, Bao Y, Wang Y, Zhao W. The GSA Family in 2025: A Broadened Sharing Platform for Multi-omics and Multimodal Data. Genomics Proteom Bioinf. 2025;23(4):qzaf072. https://doi.org/10.1093/gpbjnl/qzaf072. PMID: 40857552; PMCID: PMC12451262.
44. CNCB-NGDC Members and Partners. Database Resources of the National Genomics Data Center, China National Center for Bioinformation in 2025. Nucleic Acids Res. 2025;53(D1):D30–44. https://doi.org/10.1093/nar/gkae978. PMID: 39530327; PMCID: PMC11701749.

Publisher's Note